Structural Monitoring and Maintenance, *Vol. 11, No. 2 (2024) 149-171*
https://doi.org/10.12989/smm.2024.11.2.149

Theoretical and practical discussion of drive-by monitoring of railway bridges using in-service vehicles

Achraf Zouizza* and Malika Azmi

Ecole Hassania des Travaux Publics, Casablanca, Morocco

(*Received May 4, 2024, Revised June 10, 2024, Accepted June 20, 2024*)

Abstract. Drive-by monitoring (also known as indirect monitoring or mobile sensing) of bridges has obvious advantages when compared to other approaches of Structural Health Monitoring. The underlying concept involves leveraging the coupling between the vertical vibrations of the bridge and those generated in the passing vehicle. In this scenario, the vehicle serves as both the initiator and recipient of the vibrations, which can provide information on the structural condition of the bridge. In the literature, a wide range of methods has been proposed, primarily focused on highway bridges. However, limited research has been published to assess the suitability of indirect methods for monitoring railway bridges, bounded to numerical studies based on theoretical simulations and, rarely, on experimental investigations. The aim of this work is to contribute to filling this gap and explore the feasibility of implementing drive-by monitoring for railway bridges using in-service vehicles and discuss its potential applicability, from theoretical and practical point of view, with illustration through real case studies from the Moroccan railway network.

Keywords: drive-by monitoring; railway bridges; sensors, structural damage; structural health monitoring; vibrations

1. Introduction

Structural Health Monitoring (SHM) is a necessity to ensure the long-term performance of bridges. In fact, the load-bearing capacity of these structures and their serviceability can deteriorate, due to several factors such as intensive use, general trend to increase speed and axle loads, environmental conditions and aging. In this context, it is vital to record and analyse the state of the infrastructure in a periodic way, in order to make safety statements, service life forecasts, and schedule maintenance measures.

Traditional surveillance programs set up by infrastructure managers are mainly based on visual inspection, depending on the experience of the inspector and his level of vigilance. Due to the large number of bridges assets, the inspection visits are generally scheduled at the rate of one visit per year, or shorter periodicity for “acceptably” damaged bridges. Besides, these inspections are not only costly in terms of budget; they are also highly time consuming. Furthermore, in several cases, some parts of the structure are not reachable by the inspector without resorting to special means such as scaffolding, positive or negative nacelles, drones, ... such parts are whether situated

*Corresponding author, Ph.D. Student, E-mail: zouizza.achraf.cedoc@ehtp.ac.ma

http://www.techno-press.org/?journal=smm&subpage=7 ISSN: 2288-6605 (Print), 2288-6613 (Online)

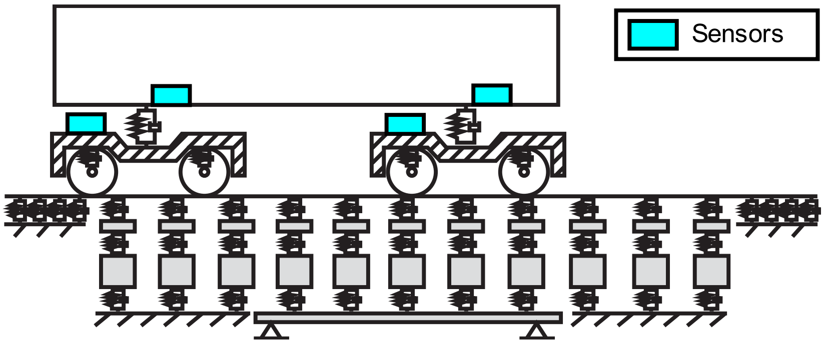

Fig. 1 Principle of indirect monitoring of a railway bridge

at important height, hided by the presence of vegetation, or placed over a watercourse. Even climatic conditions at the moment of the inspection can be decisive (wind, precipitations, solar rays' orientation). In the past few decades, there has been a growing interest among engineers in employing direct structural health monitoring (SHM) methods, in which special instrumentation is installed on the site in order to perform real-time monitoring of significant quantities: accelerations, displacements, inclinations, stresses, strains, temperature, etc. In particular, vibration-based SHM of bridges (VbSHM) began to be widely used (Akbari *et al*. 2023, Azhar *et al*. (2024). However, the installation and maintenance of the sensors generate considerable expenses, which makes it impractical to equip the large number of bridges in the conventional network.

For these reasons, there is a natural residual risk of undetected damage, whose discreet appearance and evolution would cause the abrupt collapse of the structure with eventual losses of human lives. In certain instances, the presence of damage may necessitate extensive repair or reinforcement work, or even the complete demolition and subsequent replacement of the structure. These actions can result in significant additional costs and disruptions to regular traffic flow, which could have been mitigated if the damage had been detected at an earlier stage.

The alternative solution that we propose to study consists in analyzing the dynamic response of an instrumented vehicle as it passes over bridges (Fig. 1). This method has the potential to optimize and make the monitoring of the bridges asset more reliable, since it is a solution that is (Zouizza and Azmi 2022):

- fundamentally straightforward to implement;
- providing the potential for continuous and near-permanent monitoring;
- objective, relying on measurements, mitigating the subjectivity of human judgment;
- ensuring no disruption to traffic, as the inspection is conducted onboard an in-service vehicle;
- cost-effective, involving acquiring, installing, and maintaining sensors on the vehicles specifically intended for this purpose.

In light of these positive features, indirect monitoring of bridges, by capturing their dynamic response through sensors installed on a passing vehicle, has garnered the attention of numerous researchers (Malekjafarian *et al*. 2022), especially in the case of road bridges (Benedetti *et al.* 2022, Lan *et al.* 2023). The proposed approaches can be categorized into two main groups (Malekjafarian *et al*. 2022):

(a) Bridge modal identification methods in which the main focus is finding the bridge modal parameters, such as natural frequencies, damping ratios and mode shapes.

(b) Bridge condition monitoring methods which process the measured vehicle responses (e.g., axle acceleration) to assess the bridge condition.

Despite being demonstrated at a theoretical level and in a few limited experiments, these methods encounter several challenges that hinder their practical implementation (Zouizza and Azmi 2022):

- Typically, conducting experiments on structures that already have severe structural damage is practically challenging due to the limitations imposed by infrastructure managers;
- The majority of the proposed methods rely on simplified models for both the axle and the vehicle;
- The presence of irregularities or roughness in the pavement profile can exert a substantial influence on the recorded response;
- To minimize the impact of the pavement profile and ensure accurate identification of vibratory behavior, it is necessary to maintain limited crossing speeds;
- Due to the brief duration of the vehicle's passage over the bridge, it is essential to employ high-frequency acquisition instruments;
- The recorded signal will inevitably include noise originating from the immediate surroundings of the structure, such as wind or seismic activity;

Railway bridges, the focus of this study, entail additional complexities in comparison to road bridges:

- The analysis of the behavior of railway bridges is further complicated due to the inclusion of the railway superstructure components, such as rails, sleepers, ties, and ballast;
- Modeling railway vehicles necessitates a greater number of degrees of freedom in comparison to road vehicles;
- The behavior of the train-track-bridge system is influenced by factors such as wheel conicity and rail profile, which are challenging to control or manage effectively.

The aforementioned challenges likely contribute to the limited amount of published research assessing the potential of indirect methods for monitoring railway bridges (Malekjafarian *et al.* 2022, De Souza *et al*. 2023). Quirke *et al*. (2017) proposed a method for the detection of bridge damage through comparison of apparent profiles sensed by the passing vehicle. The apparent profile is defined as a virtual longitudinal profile which, when applied to a vehicle, invokes the same measured response to the crossing of a bridge. A change in the deflection of the bridge due to the presence of damage manifests itself as a change in the apparent profile associated with the measured vehicle response. Carnevale *et al*. (2019), through train-track-bridge simulations of different scenarios, gave a general discussion on the feasibility of drive-by inspection in the case of non-resonant bridges, outlining the main operational parameters affecting the method. In the contrast, Matsuoka *et al.* (2021) proposed a novel method to detect resonant bridges in high-speed railways, based on the difference between the track irregularities measured by the devices mounted on the first and last vehicles of the train, thus defining a Resonance Detection Index (RDI). Bernardini *et al*. (2021) performed a numerical study of a short span Warren truss bridge, simulating two kinds of defects in different working conditions and for different intensities of the damage level, and analyzed the resulting response using Continuous Wavelet and Huang-Hilbert transforms.

The next sections provide a comprehensive examination of the feasibility of drive-by monitoring for railway bridges, encompassing both theoretical and practical aspects. The investigation includes the presentation of real case studies from the Moroccan railway network to illustrate the discussed concepts.

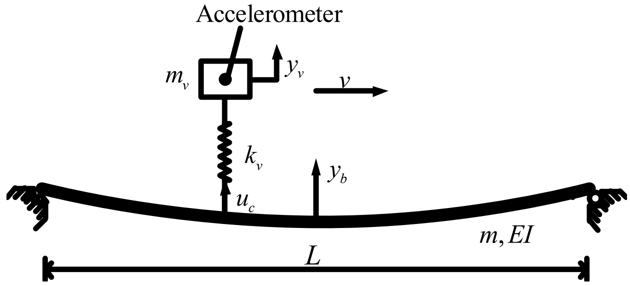

Fig. 2 Vehicle-bridge interaction simplified model (according to Yang *et al.* (2018))

2. Theoretical background

In the context of indirect monitoring, the vehicle assumes a dual role: it serves as both the exciter of the structure it traverses and the receiver of the resulting vibrations. In the literature many formulations are proposed for the vehicle-bridge interaction (VBI) dynamics (Paz and Leigh 2004, Fryba 1996, 1999, Yang *et al.* 2012, Biondi *et al.* 2005). This interaction results in a set of coupled second-degree differential equations written in the following general matrix form

$$[\mathrm{M}]\{\ddot{q}\} + [\mathrm{C}]\{\dot{q}\} + [\mathrm{K}]\{\mathrm{q}\} = \{\mathrm{F}\} \tag{1}$$

In which [M], [C] and [K] denote respectively the mass, damping and stiffness matrices, {q} is the displacement vector, {F} is the external force vector, and the dot represents the derivative with respect to time. However, a simplified model is quite satisfactory to identify the key parameters dominating the VBI response. In this context, a closed-form solution was presented by Yang *et al.* (2004, 2018, 2020) for the case of highway bridges, based on the model of a simply supported Bernoulli-Euler beam subjected to a moving sprung mass m_v supported by a spring of stiffness k_v and moving at constant speed v (Fig. 2). The beam is described by a span length L a unit mass m, an elastic modulus E, and a moment of inertia I. u and y denote the vertical displacement of the beam and the vehicle respectively.

Under some assumptions (namely neglected damping, neglected vehicle to bridge mass ratio, smooth road profile, zero initial conditions, use of modal superposition method), the vertical acceleration of the vehicle (sprung mass) is given by

$$\ddot{y}_v = \sum_{n=1}^{\infty} \frac{\Delta_{stn}}{2(1-S_n^2)} \left\{ \begin{array}{c} \dfrac{\omega_v^2\left(\frac{2n\pi v}{L}\right)^2}{\omega_v^2-\left(\frac{2n\pi v}{L}\right)^2} cos\left(\frac{2n\pi vt}{L}\right) \\ -A_n\omega_v^2 cos(\omega_v t) \\ +S_n \left[\begin{array}{c} \dfrac{\omega_v^2\left(\omega_{bn}-\frac{n\pi v}{L}\right)^2}{\omega_v^2-\left(\omega_{bn}-\frac{n\pi v}{L}\right)^2} \\ * cos\left(\omega_{bn}-\frac{n\pi v}{L}\right)t \\ -\dfrac{\omega_v^2\left(\omega_{bn}+\frac{n\pi v}{L}\right)^2}{\omega_v^2-\left(\omega_{bn}+\frac{n\pi v}{L}\right)^2} \\ * cos\left(\omega_{bn}+\frac{n\pi v}{L}\right)t \end{array} \right] \end{array} \right\} \tag{2}$$

And the contact point vertical acceleration is yielded as

$$\ddot{u}_c = \sum_{n=1}^{\infty} \frac{\Delta_{stn}}{2(1-S_n^2)} \left\{ \begin{array}{c} \left(\frac{2n\pi v}{L}\right)^2 cos\left(\frac{2n\pi vt}{L}\right) \\ +S_n \left[\begin{array}{c} \left(\omega_{bn} - \frac{n\pi v}{L}\right)^2 \\ * \, cos\left(\omega_{bn} - \frac{n\pi v}{L}\right) t \\ -\left(\omega_{bn} + \frac{n\pi v}{L}\right)^2 \\ * \, cos\left(\omega_{bn} + \frac{n\pi v}{L}\right) t \end{array} \right] \end{array} \right\} \tag{3}$$

Where ω_v denotes the vehicle frequency and ω_{bn} the nth bridge frequency

$$\omega_v = \sqrt{\frac{k_v}{m_v}} \tag{4}$$

$$\omega_{bn} = \left(\frac{n\pi}{L}\right)^2 \sqrt{\frac{EI}{m}} \tag{5}$$

Δ_{stn} is approximately the nth modal static deflection of the midspan of the beam under the gravity action

$$\Delta_{stn} = -\frac{2m_v g L^3}{EI(n\pi)^4} \tag{6}$$

S_n is the speed parameter, defined as the ratio of the half driving frequencies $\omega_{dn}/2 = n\pi v/L$ to the bridge frequencies ω_{bn}

$$S_n = \frac{n\pi v}{L\omega_{bn}} \tag{7}$$

A_n is a constant depending on the speed parameter and the frequencies of beam and vehicle

$$A_n = \frac{4{S_n}^2{\mu_n}^4(1-{S_n}^2)(2+{S_n}^2{\mu_n}^2-{\mu_n}^2)}{(4{\mu_n}^2{S_n}^2-1)\left[1-2{\mu_n}^2(1+{S_n}^2)+{\mu_n}^4(1-{S_n}^2)^2\right]} \tag{8}$$

$$\mu_n = \frac{\omega_{bn}}{\omega_v} \tag{9}$$

As can be seen from Eqs. (2) and (3), the responses of the vehicle and the contact point are dominated by the driving frequencies $\omega_{dn} = 2n\pi v/L$ and the shifted frequencies of the beam $\omega_{bn} - \omega_{dn}/2$ and $\omega_{bn} + \omega_{dn}/2$. Besides, the vehicle response is also dominated by its proper frequency ω_v, while the latter is not present in the contact point response. It is important to notice that, in Eqs. (2) and (3), the contributions of each frequency are expressed as rational functions of the order n that diminish as the order increases. As a result, the vehicle and contact point responses can be expressed in terms of the first few orders, the contribution of higher orders being insignificant.

The presented formulation has been presented for highway bridges. Its relevance lies in its simplicity and clarity in determining the key parameters of vehicle-bridge interaction. As far as railway bridges are concerned, a suitable formulation should deal with the effect of the track components (rail, fasteners, pads, sleepers and ballast) and the railway vehicle characteristics (including wheelsets, bogies, car body, primary and secondary suspensions). However, at first approximation, we can consider that the formulation above is sufficient to describe railway vehicle-bridge interaction if we admit that the railway peculiarities are indirectly included, provided that the values of m_v and k_v allow to get equivalent results. Moreover, given that an efficient way for indirect monitoring implementation is to use a real operating train (see section 3.1), and considering the latter as a series of sprung masses (neglecting pitch, yaw and roll effects), other significant frequencies should be expected in the response's spectrum, depending on the train speed and its characteristic distances: car length l_c, bogies spacing within a car l_b, and wheelsets spacing within a bogie l_w. In particular, it was demonstrated (Milne *et al.* 2017) that the sleeper velocity spectrum is dominated by integer multiples of the passing frequency, defined as the ratio between the train speed and the car length (i.e., v/l_c).

All previous conclusions are based on idealized models and simplifying assumptions, unrepresentative of real behavior of the train-track-bridges interactions dynamics. It is then necessary to study the aforementioned spectral features through real case studies and discuss the feasibility of drive-by monitoring applications, which is the object of the next sections.

3. Real conditions of drive-by monitoring implementation

3.1 Monitoring vehicle

To capitalize on the advantages offered by indirect monitoring approaches applied to railway bridges, real operating train fleets should be used, instead of vehicles specially dedicated and programmed for this purpose (such as the EM120, the machine employed to assess the track and catenary quality of the Moroccan network), so as not to disturb the normal course of commercial traffic. In fact, utilizing a dedicated vehicle can pose challenges in terms of traffic capacity, as is often the case with railway maintenance operations employing specialized machines (Lidén 2015).

For more efficiency and reliability, it is recommended to carry out experiments on all the vehicles asset in order to choose the most adequate ones in terms of dynamic response (especially predominant frequencies and signal-to-noise ratio) in various levels of speed. The primary criterion should be the sensitivity of the recorded response to the dynamics of the bridges.

In this context, it is important to mention that the feasibility and accuracy of the aforementioned methods must be established for each railway network, depending not only on the types of vehicles circulating on it and their dynamic parameters, but also on the maintenance strategies in which the frequency of interventions (planning of tamping, lining/levelling, grinding works) as well as that the tolerances of the track geometrical characteristics can differ noticeably, not to mention substantial matters such as the track gauge.

In this respect, the present paper deals with drive-by monitoring involving trains of the Moroccan network, whose exploitation and maintenance is ensured by the *Office National des Chemins de Fer (ONCF)*. The results and conclusions inferred can be extended to similar networks with regard to the mentioned aspects.

3.2 Monitoring schedule

The objective of the infrastructure manager is to be able to monitor all of his bridge assets in a quasi-continuous manner and to be able to draw the relevant conclusions in order to carry out the necessary actions in a timely manner. With this in mind, the monitoring program and the choice of trains to be instrumented must take into account the normal flow of traffic so as to encompass all lines of the network.

A priori, when using in-service trains in drive by monitoring, there is no limit to the scheduling possibilities. However, two main concerns need to be addressed: the first is related to the huge amount of data acquired during indirect monitoring: depending on the quantity and the quality of the utilized sensors, the storage and processing of the recorded data may be a real challenge; The second issue is related to the state of the track and trains, which deteriorates over time, leading to a diminished quality of the rail-wheel contact. As a consequence, this significantly affects the vibratory response recorded in the vehicle. One potential solution would be to plan the monitoring immediately after scheduled maintenance operations on the track and rolling stock have been carried out. Whitin this framework, it is advisable to make use of the favorable conditions encountered during comfort measurement campaigns, which are routinely conducted by railway infrastructure managers (in Europe, these campaigns are carried out according to the standard EN 12299).

The data analyzed in the present paper is taken from the raw recordings of the comfort measuring campaign led by the ONCF in 2018. The aim is to examine to what extent the same recorded data, originally intended to assess the comfort of passengers on board trains, can be used for structural health monitoring of crossed railway bridges during the campaign.

The instrumented car was a *"Coach"* passenger car, identical to *"Corail"* passenger cars of the *SNCF*, the French railway company (weight 41 tons, length 26.40 m, wheelbase 18.30 m, bogies type Y 32 A, bogie wheelbase 2.56 m). It was checked during a technical inspection before the measurement campaign. During the measurements, no traveler was present in the car. This way the recordings will not be affected by the activity of the travelers. However, it is possible that some limited disturbances were recorded because of the movement of the technical staff.

3.3 Instrumentation

The instrumentation to be deployed should possess an adequate level of accuracy to effectively capture and record vehicle accelerations and its position over time. In the present study, the instrumentation installed on the chosen car is composed of (Fig. 3):

- Triaxial accelerometers on the bogie (axle, bogie frame, car body)
- Triaxial accelerometers on the base of the passenger seats inside the car (second, tenth and seventeenth rows of seats counting from the front of the car to the rear)
- A GPS system and a tachymeter for speed measurement, synchronized with acceleration recordings.

Special attention should be accorded to the choice of the accelerometers, the master pieces in the monitoring vehicle equipment. One of the key parameters of an accelerometer is the sampling frequency. The latter should not be less than twice the maximum frequency that is to be recorded, as stated by the Nyquist-Shannon sampling theorem. In this respect, it should be noted that, in the vertical direction, the typical frequency range of railway vehicle motions due to track characteristics, suspensions, as well as wheel defects and the instrumentation to be deployed should possess an adequate level of accuracy to effectively capture and record vehicle accelerations and its position over time. In the present study, the instrumentation installed on the chosen car is composed of (Fig. 3):

- Triaxial accelerometers on the bogie (axle, bogie frame, car body)
- Triaxial accelerometers on the base of the passenger seats inside the car (second, tenth and seventeenth rows of seats counting from the front of the car to the rear)
- A GPS system and a tachymeter for speed measurement, synchronized with acceleration recordings.

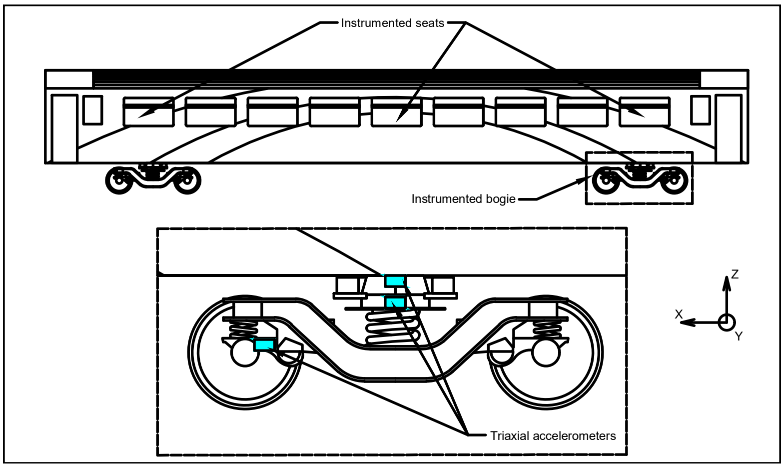

Fig. 3 Location of accelerometers on the monitoring vehicle

Special attention should be accorded to the choice of the accelerometers, the master pieces in the monitoring vehicle equipment. One of the key parameters of an accelerometer is the sampling frequency. The latter should not be less than twice the maximum frequency that is to be recorded, as stated by the Nyquist-Shannon sampling theorem. In this respect, it should be noted that, in the vertical direction, the typical frequency range of railway vehicle motions due to track characteristics, suspensions, as well as wheel defects and vehicle body modes, is up to 40 Hz. In the transverse direction, these movements, in addition to those due to the pitch, roll and yaw modes of the vehicle body, have a frequency range up to 15 Hz (EN 12229). Moreover, the upper bound of the first driving frequency range can reach 4.4 Hz for bridges having more than 10 m span length traversed at a 160 km/h speed (maximal speed in the Moroccan conventional network). As a result, accelerometers with 40-50 hz sampling frequency are generally sufficient for the needs of drive-by monitoring. The accelerometers used in the present study are triaxial piezoelectric accelerometers, model 356A02, with 10 mV/g sensitivity and a 2048 Hz sampling frequency.

In the following sections, focus will be made on vertical accelerations recorded at the axle, the bogie frame and the car body.

3.4 Extraction of bridges recordings

The first challenge encountered, using a train in normal service as an exciter-receiver, is the detection of the recording that corresponds to the bridges under study. In fact, as can be seen in Figs. 4 to 6, the signal recorded is too noisy and the windows corresponding to bridges are not visually distinguishable as it may be expected, due to the relative flexibility of the bridges decks when compared to earthworks. A clear relationship can be noted between the acceleration amplitude and the train speed (Fig. 7).

The use of Global Positioning System (GPS) receivers alone does not solve this issue because their accuracy may be affected by a variety of factors (the quality of the GPS receiver, the number and positioning of satellites in view, the presence of obstacles or interference, and the processing algorithms used, challenging environments like dense urban areas with tall buildings, deep valleys, or dense forests.

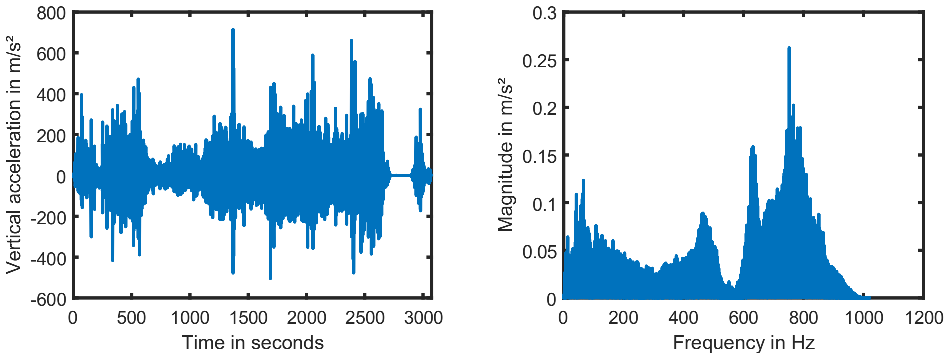

Fig. 4 Recorded vertical acceleration at the left side of the rear axle in time and frequency domains during the whole journey

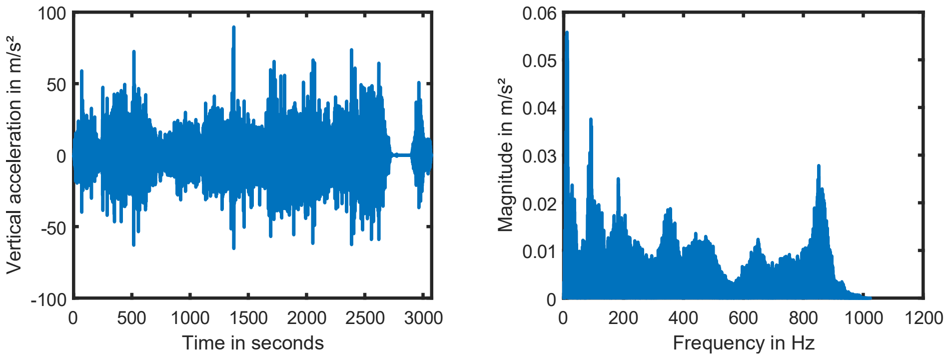

Fig. 5 Recorded vertical acceleration at the left side of the rear bogie frame in time and frequency domains during the whole journey

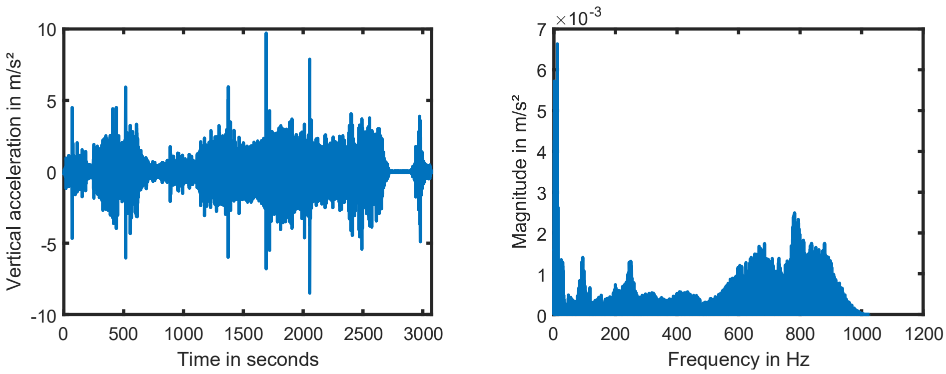

Fig. 6 Recorded vertical acceleration at the left side of the rear car body in time and frequency domains during the whole journey

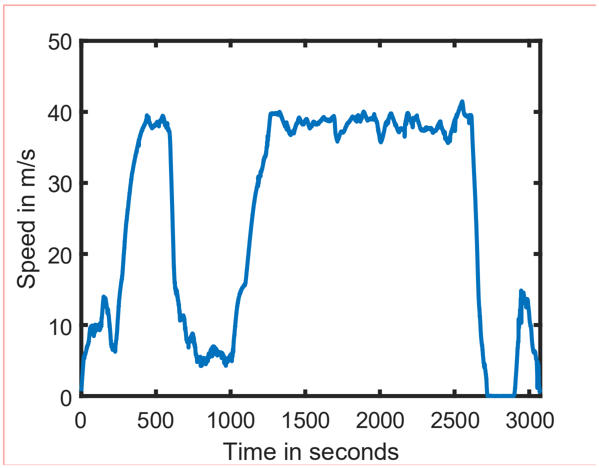

Fig. 7 Train speed during the whole journey

To address this issue, one solution would be to know beforehand the position of bridges (start – end) relative to reference points (stations, switches, expansion devices, …), preferably whose signature may be easily found in the recording, use a tachymeter to record the speed evolution from these points, and then get the location of bridges on the recording by simple temporal integration of the speed. This method can be combined with the drawing of signal peaks (envelope of the signal) and analyzing their tendency. As a side-note, the milestones installed along the track do not reflect the real distance from the origin of the railway line: they only give an approximate position on the line.

Another method that showed good identification of bridges recordings is the use of empirical mode decomposition (EMD). Applied to a signal "surrounding" the bridge under study (extracted based on GPS data), with a length equivalent to at least three times the span or length of the bridge – determined by the mean value of speed -, the bridge delimitation is clearly identified in the time history of the intrinsic mode function (IMF) whose spectrum is dominated by the first corresponding driving frequency ω_{d1}, with good adjustment of EMD parameters.

4. Case studies

In this section, we will focus on the responses recorded when crossing seven (7) railway bridges of the Moroccan railway network. For confidentiality reasons, these bridges will be simply numerated, and their location will not be mentioned.

Bridges #1 to #4 (Fig. 8) were chosen because of their similarity (they have the same cross section, the same span lengths both for edge and intermediate spans, and they've even been constructed by the same contractor, in the same period). The rest of bridges were considered to assess different conditions of spans and transit speed.

All the bridges studied have a reinforced concrete deck. The mechanical system is that of a simply supported Euler-Bernoulli beam, which represents most bridges encountered in the field. Tables 1 gives the main mechanical and geometrical characteristics of the latter, and theoretical predominant frequencies are presented in Table 2.

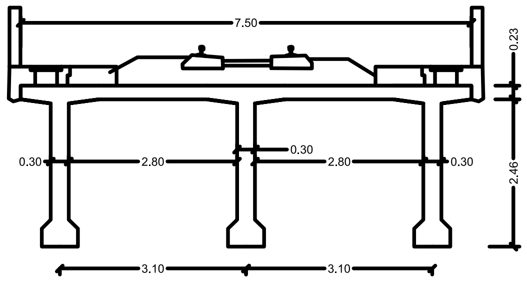

Fig. 8 Typical cross section of bridge #1 to #4

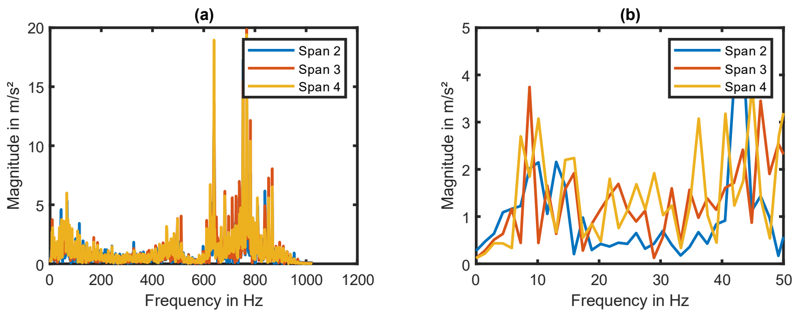

Fig. 9 FFT of vertical acceleration at the left side of the rear axle while crossing bridge #1: (a) entire spectrum, and (b) zoom on the range 0Hz – 50 Hz

Table 1 Main geometrical and mechanical properties of the studied bridges with crossing speed during operation

	Span length L (m)	Modulus of elasticity E (GPa)	Moment of inertia I (m^4)	Mass per unit length μ (T/m)	Train crossing speed V (km/h)
Bridge #1	27,50	32,00	3,76	10,95	143,14
Bridge #2	27,50	32,00	3,76	10,95	141,98
Bridge #3	27,50	32,00	3,76	10,95	120,60
Bridge #4	27,50	32,00	3,76	10,95	134,93
Bridge #5	14,00	32,00	0,77	14,46	54,50
Bridge #6	11,30	30,50	0,14	7,15	28,37
Bridge #7	14,72	30,50	0,77	13,76	95,83

4.1 Data processing

Signals corresponding to the studied bridges are extracted as described in section 3.4. These signals are processed using Fast Fourier Transform (FFT). Considering the energy content of high frequencies, and in order to preserve all the information embedded in the signals, no filtering technique is applied. Instead, a mere "zoom" on the interesting range of frequencies is performed in the raw signals' spectrums, i.e., 0 Hz – 50 Hz (note that the upper bound is slightly overestimated). The obtained spectrums are given in Figs. 9 to 29.

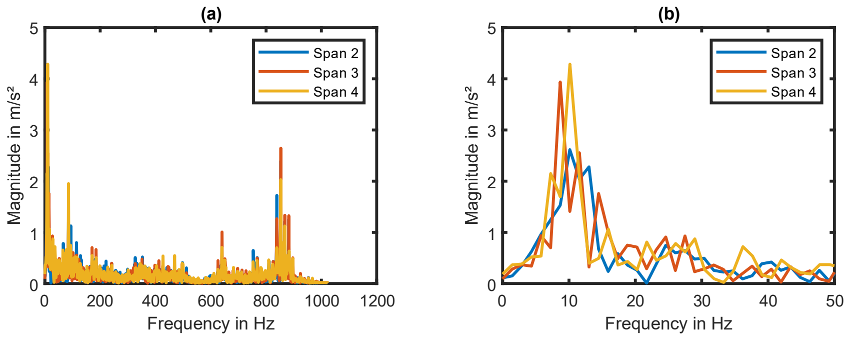

Fig. 10 FFT of vertical acceleration at the left side of the rear bogie frame while crossing bridge #1: (a) entire spectrum, and (b) zoom on the range 0Hz – 50 Hz

Table 2 Theoretical predominant frequencies in the response of the studied bridges according to Yang *et al.* (2004), Yang *et al*. (2018) and Yang *et al*. (2020)

	Order	Bridge frequency ω_{bn} in Hz	Driving frequency ω_{dn} in Hz	Left shifted bridge frequency ω_{bn}-ω_{dn}/2 in Hz	Right shifted bridge frequency ω_{bn}+ω_{dn}/2 in Hz
Bridge #1	1	6,89	1,45	6,17	7,61
	2	27,55	2,89	26,11	29,00
	3	61,99	4,34	59,82	64,16
	4	110,21	5,78	107,32	113,10
Bridge #2	1	6,89	1,43	6,17	7,61
	2	27,55	2,87	26,12	28,99
	3	61,99	4,30	59,84	64,14
	4	110,21	5,74	107,34	113,08
Bridge #3	1	6,89	1,22	6,28	7,50
	2	27,55	2,44	26,33	28,77
	3	61,99	3,65	60,17	63,82
	4	110,21	4,87	107,77	112,65
Bridge #4	1	6,89	1,36	6,21	7,57
	2	27,55	2,73	26,19	28,92
	3	61,99	4,09	59,95	64,04
	4	110,21	5,45	107,48	112,93
Bridge #5	1	10,47	1,08	9,93	11,01
	2	41,89	2,16	40,81	42,98
	3	94,26	3,24	92,64	95,88
	4	167,58	4,33	165,41	169,74
Bridge #6	1	9,59	0,70	9,24	9,94
	2	38,36	1,39	37,66	39,06
	3	86,31	2,09	85,27	87,36
	4	153,45	2,79	152,05	154,84
Bridge #7	1	9,49	1,81	8,59	10,40
	2	37,97	3,62	36,17	39,78
	3	85,44	5,43	82,73	88,15
	4	151,90	7,23	148,28	155,51

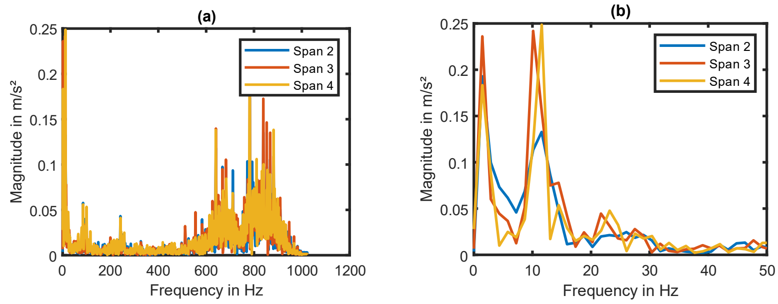

Fig. 11 FFT of vertical acceleration at the left side of the rear car body while crossing bridge #1: (a) entire spectrum, and (b) zoom on the range 0Hz – 50 Hz

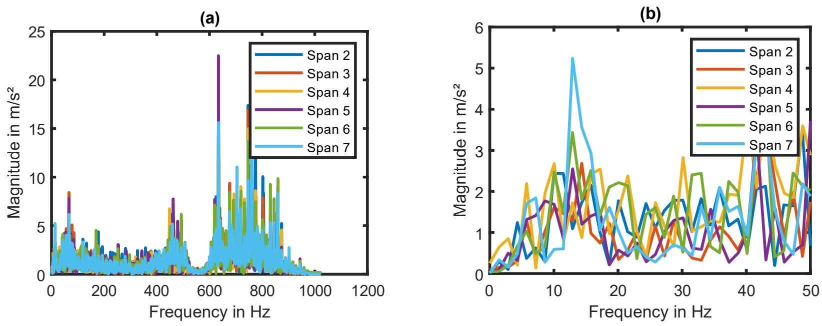

Fig. 12 FFT of vertical acceleration at the left side of the rear axle while crossing bridge #2: (a) entire spectrum, and (b) zoom on the range 0 Hz – 50 Hz

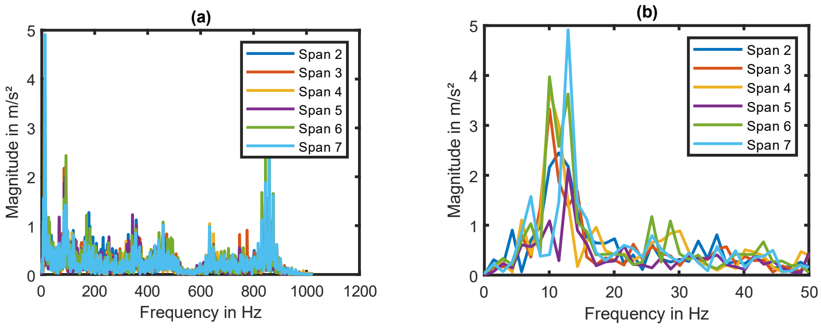

Fig. 13 FFT of vertical acceleration at the left side of the rear bogie frame while crossing bridge #2: (a) entire spectrum, and (b) zoom on the range 0 Hz – 50 Hz

4.2 Discussion and conclusions

As it would be expected, analysis in time and frequency domains of the acquired data in real environment shows clearly a poor signal-to-noise ratio. In fact, the condition of the used rolling stock (in particular the quality of suspensions of the car as well as wheel defects) and of the

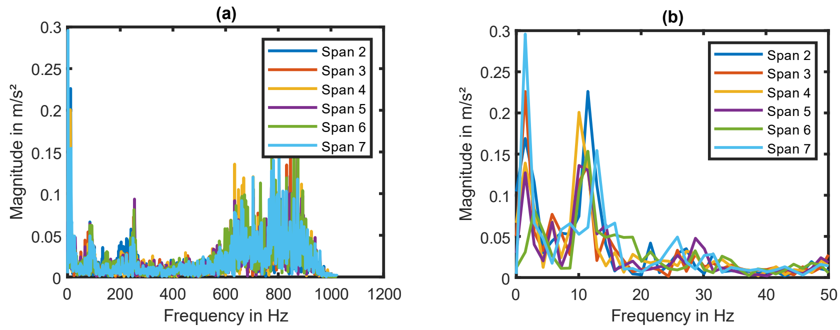

Fig. 14 FFT of vertical acceleration at the left side of the rear car body while crossing bridge #2: (a) entire spectrum, and (b) zoom on the range 0 Hz – 50 Hz

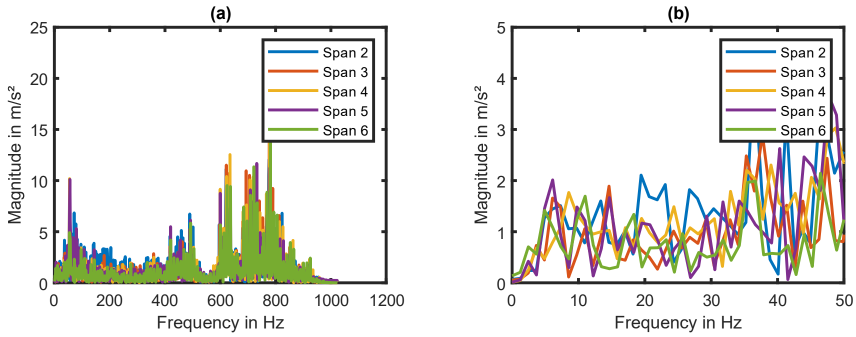

Fig. 15 FFT of vertical acceleration at the left side of the rear axle while crossing bridge #3: (a) entire spectrum, and (b) zoom on the range 0 Hz – 50 Hz

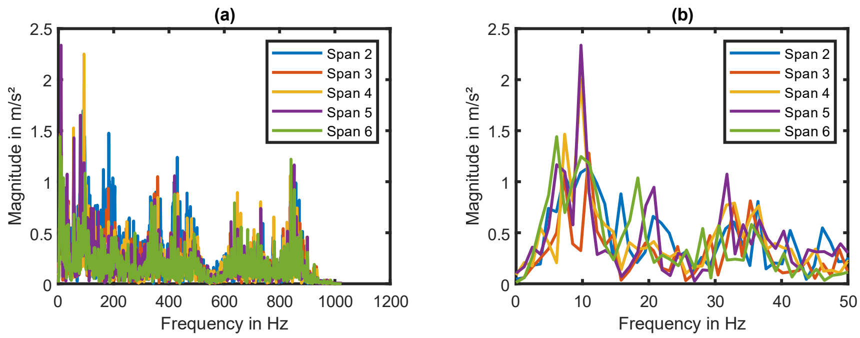

Fig. 16 FFT of vertical acceleration at the left side of the rear bogie frame while crossing bridge #3: (a) entire spectrum, and (b) zoom on the range 0 Hz – 50 Hz

railway track (ballast stiffness, irregularities, rail defects) have a strong impact on the recorded vibratory behavior. This impact can be clearly observed in the spectrums of the whole journey signals (Figs. 4 to 6), which illustrate the global characteristics of the track and train dynamics, bridges being considered mere points in the railway line.

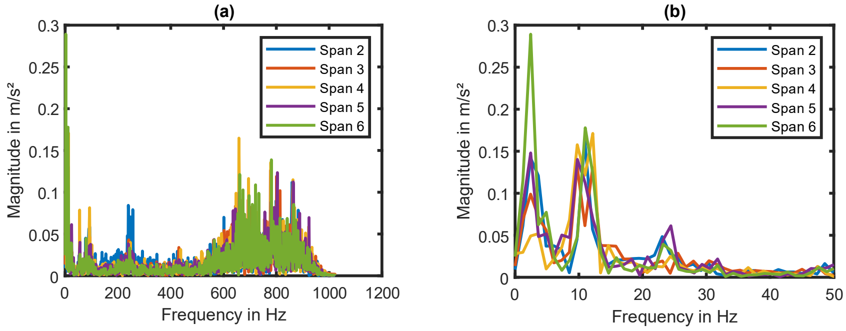

Fig. 17 FFT of vertical acceleration at the left side of the rear car body while crossing bridge #3: (a) entire spectrum, and (b) zoom on the range 0 Hz – 50 Hz

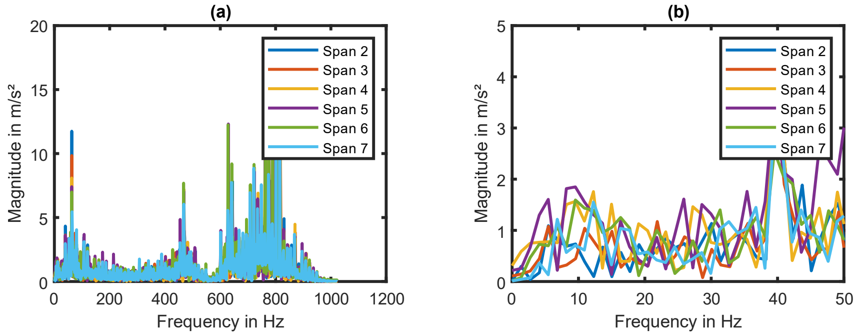

Fig. 18 FFT of vertical acceleration at the left side of the rear axle while crossing bridge #4: (a) entire spectrum, and (b) zoom on the range 0 Hz – 50 Hz

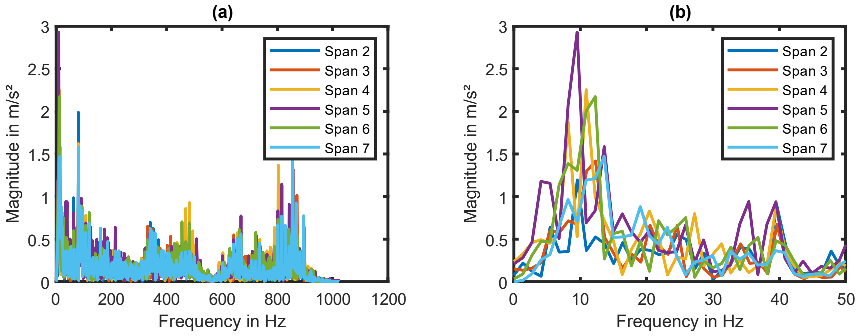

Fig. 19 FFT of vertical acceleration at the left side of the rear bogie frame while crossing bridge #4: (a) entire spectrum, and (b) zoom on the range 0 Hz – 50 Hz

4.2.1 Best sensors' position

Previous works (Yang *et al.* 2018) inferred that the contact point response is generally more accurate than that of sprung masses for modal identification of bridges, because the first is free of vehicle's frequencies as shown in Eq. (3). Other works even concluded that, in the case of railway vehicles, the car body acceleration is not sensitive enough to detect a defect on the bridge (Carnevale *et al*. 2019, Amerio *et al.* 2017). The present work shows, however, that the relevant range of frequencies is overshadowed by high frequencies content in the responses of the axle (representing the contact points) and the bogie frame, while it is clearly identifiable in the car body response (Figs. 9 to 29).

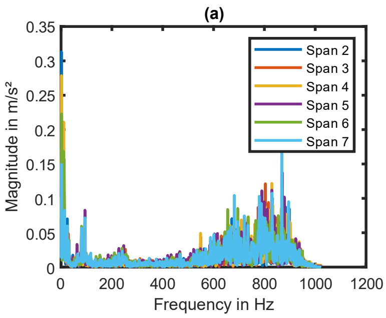

Fig. 20 FFT of vertical acceleration at the left side of the rear car body while crossing bridge #4: (a) entire spectrum, and (b) zoom on the range 0 Hz – 50 Hz

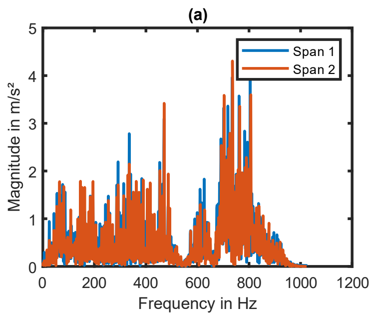

Fig. 21 FFT of vertical acceleration at the left side of the rear axle while crossing bridge #5: (a) entire spectrum, and (b) zoom on the range 0 Hz – 50 Hz

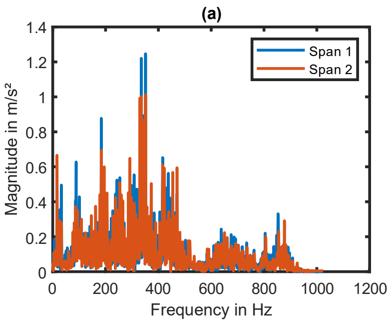

Fig. 22 FFT of vertical acceleration at the left side of the rear bogie frame while crossing bridge #5: (a) entire spectrum, and (b) zoom on the range 0 Hz – 50 Hz

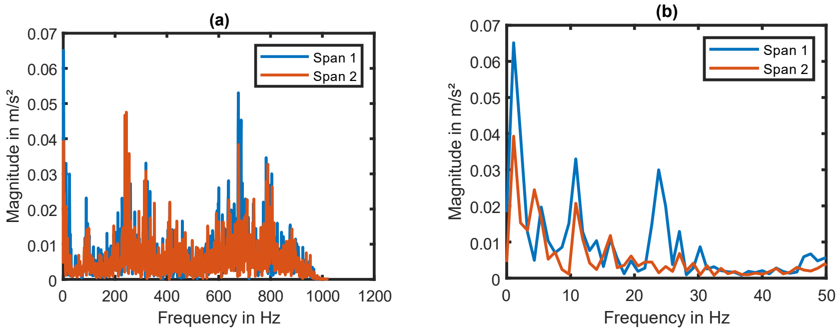

Fig. 23 FFT of vertical acceleration at the left side of the rear car body while crossing bridge #5: (a) entire spectrum, and (b) zoom on the range 0 Hz – 50 Hz

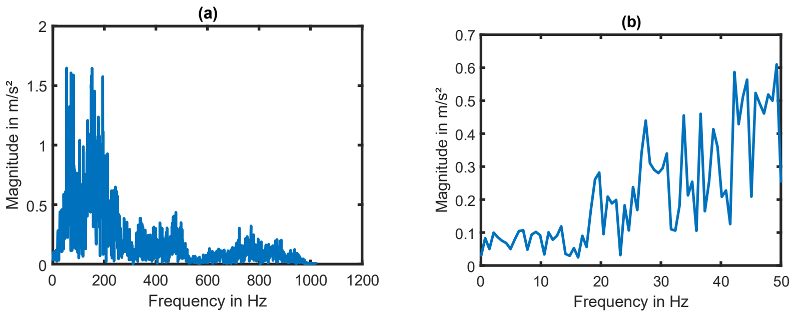

Fig. 24 FFT of vertical acceleration at the left side of the rear axle while crossing bridge #6: (a) entire spectrum, and (b) zoom on the range 0 Hz – 50 Hz

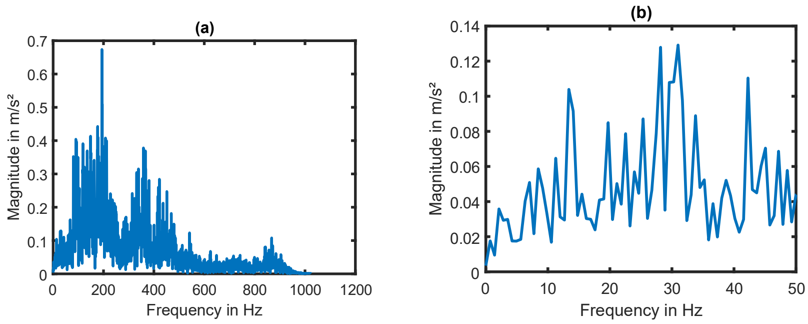

Fig. 25 FFT of vertical acceleration at the left side of the rear bogie frame while crossing bridge #6: (a) entire spectrum, and (b) zoom on the range 0 Hz – 50 Hz

4.2.2 Natural frequency as SHM indicator

In this section, the potential of natural frequency monitoring is evaluated from two aspects: First, the theoretical impact of a local damage on natural frequencies of a bridge is examined. Second, the vehicle response is analyzed with respect to the possible extraction of these frequencies.

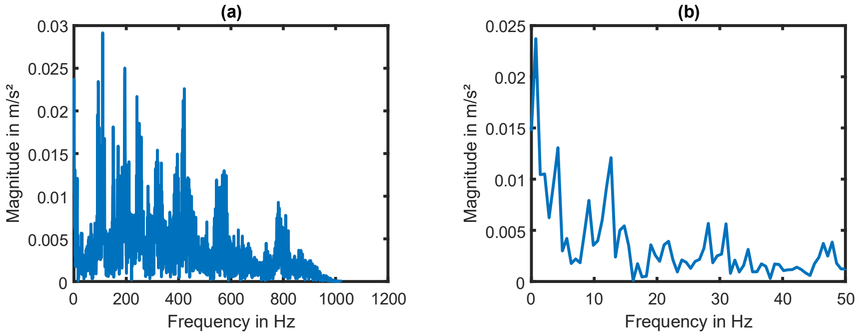

Fig. 26 FFT of vertical acceleration at the left side of the rear car body while crossing bridge #6: (a) entire spectrum, and (b) zoom on the range 0 Hz – 50 Hz

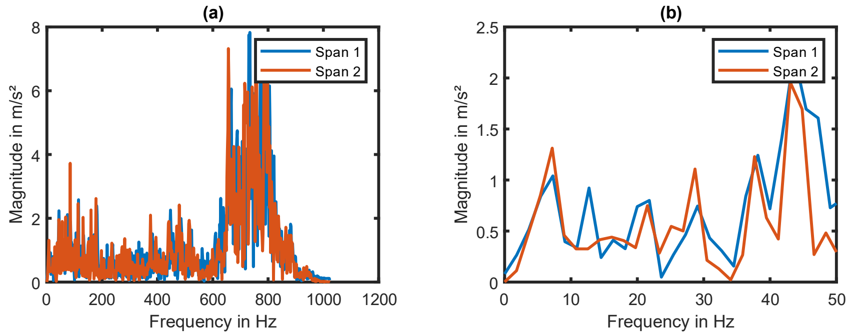

Fig. 27 FFT of vertical acceleration at the left side of the rear axle while crossing bridge #7: (a) entire spectrum, and (b) zoom on the range 0 Hz – 50 Hz

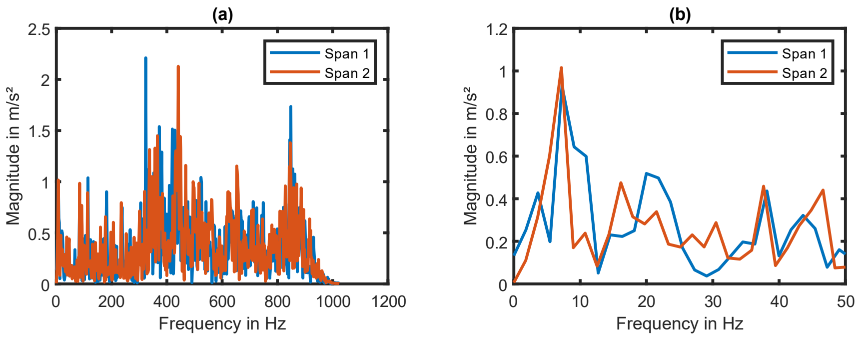

Fig. 28 FFT of vertical acceleration at the left side of the rear bogie frame while crossing bridge #7: (a) entire spectrum, and (b) zoom on the range 0 Hz – 50 Hz

From a theoretical point of view, it is necessary to assess the reduction of natural frequencies in the presence of damage. For this purpose, the studied bridges are considered as Euler-Bernoulli simply supported beams. To model the damage, the method proposed by Sinha *et al*. (2002) is

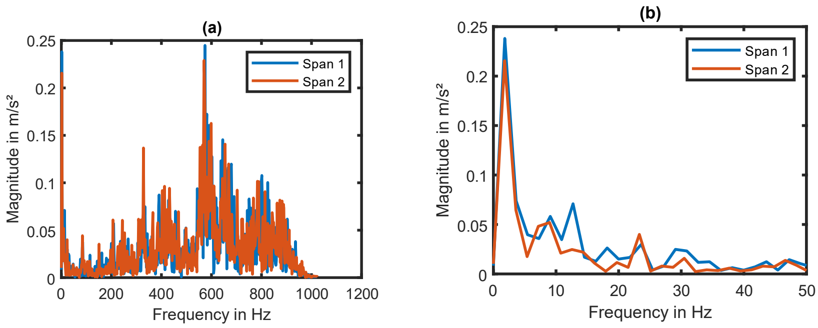

Fig. 29 FFT of vertical acceleration at the left side of the rear car body while crossing bridge #7: (a) entire spectrum, and (b) zoom on the range 0 Hz – 50 Hz

adopted: the damage is assimilated to a loss of stiffness which decreases linearly over a length of 1.5h on both sides of its location, h being the depth of the beam. This method offers the benefit of simplifying the Christides and Barr's analytical approach (Christides and Barr 1984), which is practical for finite element formulation of the problem.

As explained in section 2, the contribution of high order natural frequencies in insignificant. For this reason, only the first four eigen modes are explored in the present work. Besides, only the case of a single local damage is studied.

A program implemented on MATLAB is used to carry out the calculations. To achieve higher precision, the beam is divided into smaller elements with reduced length. These elements retain the mechanical properties of the intact structure, except for the sections representing damage. In the case of damaged sections, their stiffness is progressively decreased based on the chosen method.

Fig. 30 depicts the variation of natural frequencies with respect to damage severity and damage relative location, in the case of bridges #1 to #4. Similar values were obtained for the remaining bridges, although the corresponding figures have not been included in this paper to maintain its conciseness. It is noted that for a given damage severity, the frequency variation portrays the shape of the absolute value of the corresponding mode. Stated differently, for the same severity, the frequency reduction is more notable for damage positions which are close to the peaks of the corresponding mode, and it remains minimal near the canceling points of the latter. More explicitly, the first natural frequency is sensitive to damages around mid-span (typically flexural cracks) while it is hardly affected by damages near the supports (such as shear cracks). In the same way, the second natural frequency is sensitive to damages around quarter-span, and unresponsive the damages at mid-spans.

Furthermore, it is worth noting that the reduction in natural frequencies due to damage remains relatively minimal, especially when considering the primary goal of detecting the damage at its early stages of development. For example, the first natural frequency of bridges #1 to #4, subjected to a local damage at mid-span, is reduced by 3.65% for a 20% severity, 5.62% for a 30% severity, and 8.05% for a severity of 40%. For the same bridges, subjected to a local damage at quarter-span, the second natural frequency is reduced by 6.69% for a 40% severity, which is already a worrying value in damage evolution, considering the typical safety factors taken into account in bridge's design practice.

The direct corollary is that, for an efficient indirect monitoring based on natural frequencies, and to gain a more comprehensive understanding of the structural condition, it is crucial to extract

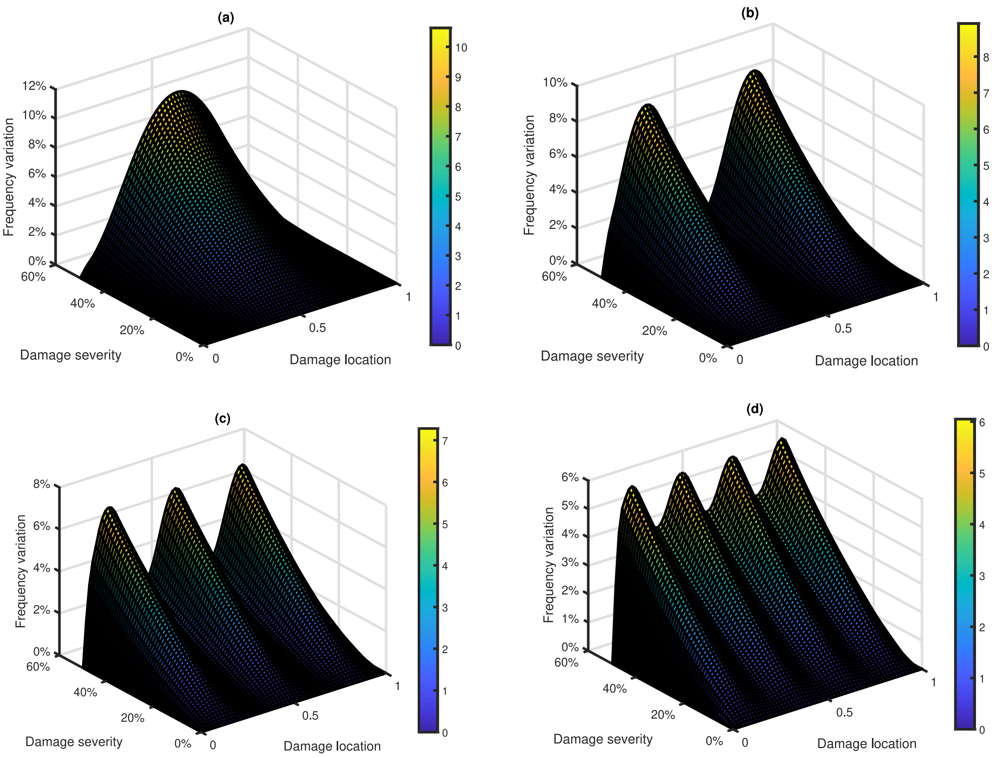

Fig. 30 Natural frequency variation with respect to damage location and severity for bridges #1 to #4: (a) 1st mode, (b) 2nd mode, (c) 3rd mode, and (d) 4th mode

as many natural frequencies as possible looking for all probable positions of damage, and to make sure that the extraction process is sensitive enough to the latter's variation.

That said, the measurements carried out in the present study show that it is unlikely to extract frequencies of order greater than or equal to 2. Only the 1st mode could be identified at low speeds based on the shifted frequencies, as can be seen for bridges #5 to 7.

For high crossing speeds (bridges #1 to 4), the natural frequencies of the structure are not clearly identifiable in the calculated spectrums, hence the interest in programming low speed crossings to be able to follow the evolution of these parameters. It is also worth emphasizing that the bridges characteristics in tables 1 and 2 are calculated based on theoretical assumptions and not on field testing or measurement. To address this issue, it is recommended to perform multiple crossings on the bridge under study, in order to get a statistically acceptable value of the actual natural frequency to be monitored in the next campaigns

4.2.3 Driving frequency (quasi-static frequency) as SHM indicator

From the drawn spectrums (Figs. 9 to 29), it is clear that the driving frequency (also known as the quasi-static frequency) can be extracted with a good accuracy for all the bridges / spans under study, including those which are crossed with relatively high velocity (bridges #1 to 4). As inferred by previous studies (Carnevale *et al*. 2019), monitoring the associated amplitude in the spectrum is

Fig. 31 Examples of cracks observed on some of the bridges under study at the time of the recording (Note that the bridges in question are subject to special monitoring conducted by the ONCF services)

considered to assess the health condition of the structure. Nevertheless, the spectrums relative to multi-spans bridges (i.e., bridges #1 to #5, and #7) show differences in the amplitudes corresponding to identical spans. These differences could be attributed to disparities whether in the mechanical characteristics (see previous section) or in the conditions of the spans: in fact, cracks of various sizes, openings, locations, and distributions were observed at the time of the campaign (some examples of damaged decks are presented in Fig. 31). Note that the bridges in question are subject to special monitoring conducted by the ONCF services.

Thus, the relation between the location and severity of structural damage and the spectral amplitudes of the quasi-static frequency (or driving frequency) needs more research to be established and tested. For this purpose, multiple recordings need to be conducted and thoroughly analyzed.

5. Conclusions

Commencing with a theoretical background discussion, this article delves into the practical aspects of drive-by monitoring, covering various topics such as the selection of the monitoring vehicle, the instrumentation to be installed, field operation scheduling, challenges in extracting bridge recordings, the influence of real conditions on the recorded response, comparisons between sensor positions on the monitoring vehicle, and the assessment of significant frequencies as indicators for structural health monitoring (SHM).

In fact, in order to leverage the benefits provided by indirect monitoring approaches for railway bridges, it is recommended to utilize real operating train fleets instead of specially dedicated and programmed vehicles. This approach ensures that the normal flow of commercial traffic remains undisturbed. Furthermore, when scheduling the monitoring operation, it is crucial to consider data management, as well as the condition of the network and vehicles. One potential solution is to align indirect monitoring activities with comfort measurement campaigns regularly carried out by railway infrastructure managers. Additionally, the instrumentation employed should possess a sufficient level of accuracy to enable the synchronized recording of bridge accelerations and vehicle position and speed. This ensures precise and reliable data collection during the monitoring process. Within this context, the presented case studies from the Moroccan railway network highlight the challenge of extracting the specific bridge recordings. This difficulty arises due to the low signal-to-noise ratio of the recorded vibrations, making the extraction process particularly demanding. In terms of determining the optimal sensor position on the vehicle, the car body emerges as the most accurate choice compared to the axle and bogie positions. This preference stems from the fact that the relevant frequency range for monitoring purposes is more pronounced in the car body spectrum, whereas the axle and bogie responses tend to be dominated by higher frequency content, making them less suitable for capturing the desired vibrations accurately. Regarding significant frequencies, the driving frequency (or quasi-static frequency) of the first order seems to be the most suitable for the requirements of Structural Health Monitoring (SHM). This frequency is clearly identifiable in the spectrum of the car body across all speeds investigated in the study, which represents the speed range typical of the conventional railway network. In contrast, the identification of the natural frequency becomes more challenging as the crossing speed increases.

In summary, it is important to mention that indirect monitoring approaches applied to railway bridges, in the light of the above considerations, are still in progress and need more experimentation on the field before reaching sufficient maturity. As such, these approaches should complement and not completely replace traditional investigation programs, relying on inspection visits carried out by well-trained, well-prepared and well-equipped personnel.

Acknowledgements

The authors would like to thank the support provided by the ONCF services, in particular for the provision of the recordings of the comfort campaign as well as the data relating to the railway infrastructure.

References

Akbari, R., Maadani, S. and Maalek, S. (2023), “Monitoring and performance assessment of a highway bridge via operational modal analysis”, *Struct. Monit. Maint.*, **10**(3), 191-205. https://doi.org/10.12989/smm.2023.10.3.191.

Amerio, L., Carnevale, M. and Collina, A. (2017), “Damage detection in railway bridges by means of train on-board sensors : A perspective option”, *Dynamics of Vehicles on Roads and Tracks*, 1215-1220. https://doi.org/10.1201/9781351057189-112.

Azhar, A.S., Kudus, S.A., Jamadin, A., Mustaffa, N.K. and Sugiura, K. (2024), “Recent vibration-based structural health monitoring on steel bridges: Systematic literature review”, *Ain Shams Eng. J.*, **15**, 102501. https://doi.org/10.1016/j.asej.2023.102501.

Benedetti, L., Bernardini, L., Argentino, A., Cazzulani, G., Somaschini, C. and Belloli, M. (2022), “Identification of bridge bending frequencies through drive-by monitoring compensating vehicle pitch detrimental effect”, *Struct. Monit. Maint.*, **9**(4), 305-321. https://doi.org/10.12989/smm.2022.9.4.305.

Bernardini, L., Carnevale, M. and Collina, A. (2021). “Damage identification in Warren Truss bridges by two different Time-Frequency algorithms”, *Appl. Sci.*, **11**(22), 10605. https://doi.org/10.3390/app112210605.
Biondi, B., Muscolino, G. and Sofi, A. (2005), “A substructure approach for the dynamic analysis of train-track-bridge system”, *Comput. Struct.*, **83**(28-30), 2271-2281. https://doi.org/10.1016/j.compstruc.2005.03.036.
Carnevale, M., Collina, A. and Peirlinck, T. (2019), “A feasibility study of the drive-by method for damage detection in railway bridges”, *Appl. Sci.*, **9**(1), 160. https://doi.org/10.3390/app9010160.
Christides, S. and Barr, A. (1984), “One-dimensional theory of cracked Bernoulli-Euler beams”, *Int. J. Mech. Sci.*, **26**(11-12), 639-648. https://doi.org/10.1016/0020-7403(84)90017-1.
De Souza, E.F., Bragança, C., Meixedo, A., Ribeiro, D., Bittencourt, T.N. and Carvalho, H. (2023), “Drive-by methodologies applied to railway infrastructure subsystems: A literature review-Part I: Bridges and viaducts”, *Appl. Sci.*, **13**(12), 6940. https://doi.org/10.3390/app13126940.
Fryba, L. (1996), *Dynamics of Railway Bridges.* Thomas Telford. Prague, Czech Republic.
Fryba, L. (1999), *Vibration of Solids and Structures Under Moving Loads.* Thomas Telford. Prague, Czech Republic.
Lan, Y., Li, Z., Koski, K., Fülöp, L., Tirkkonen, T. and Lin, W. (2023), “Bridge frequency identification in city bus monitoring: A coherence-PPI algorithm”, *Eng. Struct.*, **296**, 116913. https://doi.org/10.1016/j.engstruct.2023.116913.
Lidén, T. (2015), “Railway Infrastructure Maintenance - A survey of planning problems and conducted research”, *Transport. Res. Procedia*, **10**, 574-583. https://doi.org/10.1016/j.trpro.2015.09.011.
Malekjafarian, A., Corbally, R. and Gong, W. (2022), “A review of mobile sensing of bridges using moving vehicles: Progress to date, challenges and future trends”, *Structures*, **44**, 1466-1489. https://doi.org/10.1016/j.istruc.2022.08.075.
Matsuoka, K., Tanaka, H., Kawasaki, K., Somaschini, C. and Collina, A. (2021), “Drive-by methodology to identify resonant bridges using track irregularity measured by high-speed trains”, *Mech. Syst. Signal Pr.*, **158**, 107667. https://doi.org/10.1016/j.ymssp.2021.107667.
Milne, D.B., Pen, L.L., Thompson, D. and Powrie, W. (2017), “Properties of train load frequencies and their applications”, *J. Sound Vib.*, **397**, 123-140. https://doi.org/10.1016/j.jsv.2017.03.006.
Paz, M. and Leigh, W. (2004), *Structural Dynamics: Theory and Computation.* Kluwer Academic Publisher. Massachusetts, USA.
Quirke, P., Bowe, C., O’Brien, E.J., Cantero, D., Antolín, P. and Ruigómez, J.M.G. (2017), “Railway bridge damage detection using vehicle-based inertial measurements and apparent profile”, *Eng. Struct.*, **153**, 421-442. https://doi.org/10.1016/j.engstruct.2017.10.023.
Sinha, J., Friswell, M.I. and Edwards, S. (2002), “Simplified models for the location of cracks in beam structures using measured vibration data”, *J. Sound Vib.*, **251**(1), 13-38. https://doi.org/10.1006/jsvi.2001.3978.
Yang, Y., Lin, C. and Yau, J.D. (2004), “Extracting bridge frequencies from the dynamic response of a passing vehicle”, *J Sound Vib.*, **272**(3-5), 471-493. https://doi.org/10.1016/s0022-460x(03)00378-x.
Yang, Y., Wang, Z., Shi, K., Xu, H. and Wu, Y. (2020), “State-of-the-art of vehicle-based methods for detecting various properties of highway bridges and railway tracks”, *Int. J. Struct. Stab. Dyn.*, **20**(13), 2041004. https://doi.org/10.1142/s0219455420410047.
Yang, Y., Zhang, B., Qian, Y. and Wu, Y. (2018), “Contact-Point response for modal identification of bridges by a moving test vehicle”, *Int. J. Struct. Stab. Dyn.*, **18**(5), 1850073. https://doi.org/10.1142/s0219455418500736.
Yang, Y.B., Yau, J.D. and Wu, Y.S. (2012), *Vehicle-Bridge Interaction Dynamics: With Applications To High-Speed Railways*. New Jersey etc.: World Scientific.
Zouizza, A. and Azmi, M. (2022), “Drive-by monitoring of rail-bridges: A case study”, *Materials Today: Proceedings*, **58**, 1301-1307. https://doi.org/10.1016/j.matpr.2022.02.145.

JK